IEICE TRANSACTIONS

on Communications

VOL. E105-B NO. 3
MARCH 2022

A PUBLICATION OF THE COMMUNICATIONS SOCIETY

The Institute of Electronics, Information and Communication Engineers
Kikai-Shinko-Kaikan Bldg., 5-8, Shibakoen 3chome, Minato-ku, TOKYO, 105-0011 JAPAN

PAPER

A Study on Gain Enhanced Leaf-Shaped Bow-Tie Slot Array Antenna within Quasi-Millimeter Wave Band

Mangseang HOR[†a)], ***Student Member***, **Takashi HIKAGE**[†], ***and*** **Manabu YAMAMOTO**[†], ***Members***

SUMMARY In this paper, a linear array of 4 leaf-shaped bowtie slot antennas is proposed for use in quasi-millimeter wave band. The slot antennas array is designed to operate at 28 GHz frequency band. The leaf-shaped bowtie slot antenna is a type of self-complementary antenna with low profile and low cost of fabrication. The proposed antenna structure offers improvement in radiation pattern, gain, and −10 dB impedance bandwidth. Through out of this paper radiation pattern, actual gain, and −10 dB impedance bandwidth are evaluated by Finite Different Time Domain (FDTD) simulation. Antenna characteristics are analyzed in the frequency range of 27 GHz to 29 GHz. To improve antenna characteristics such as actual gain and −10 dB impedance bandwidth, a dielectric superstrate layer with relative permittivity of 10.2 is placed on top of ground plane of the slot antennas array. Three antenna structures are introduced and compared. With two layers of dielectric superstrate on top of the antennas ground plane, analysis results show that −10 dB impedance bandwidth occupies the frequency range of 27.17 GHz to 28.39 GHz. Therefore, the operational impedance bandwidth is 1.22 GHz. Maximum actual gain of the slot antennas array with two dielectric superstrate layers is 20.49 dBi and −3 dB gain bandwidth occupies the frequency range of 27.02 GHz to 28.57 GHz. To validate the analysis results, prototype of the designed slot antennas array is fabricated. Characteristics of the slot antennas array are measured and compared with the analysis results.

key words: *leaf-shaped bowtie slot antenna, slot antennas array, FDTD, quasi-millimeter wave band*

1. Introduction

The use of mobile data for smartphone application and mobile pocket Wi-Fi has rapidly increased during last decade. User has demanded more high-speed data rate for daily life such as video streaming, gaming, and video conferencing [1]. The use of mobile data is projected to significantly grow by 2030 [2], [3]. To comply with this unprecedented growth, millimeter wave frequency spectrum has been proposed and explored for potential application in the future [4]. In millimeter-wave frequency band, 28 GHz frequency band is more favorable than other proposed frequency bands. However, millimeter wave frequency spectrum is prone to atmosphere attenuation due to the short wavelength. Therefore, antenna, which is suitable for millimeter wave frequency, should have high gain to compensate free-space loss [3]. In addition, the antenna should also have a broad bandwidth to have high bit rate transfer. 2×2 square dense dielectric patch has been proposed for 28 GHz frequency band [5]. To enhance gain and improve bandwidth, a holey dielectric superstrate has been used in [5]. As the results, impedance bandwidth of the antenna structure in [5] occupies the range of 26.5 GHz to 30.8 GHz and has maximum gain of about 16 dBi [5]. Nevertheless, multilayer dielectric substrate has been used to fabricate antenna prototype in [5] and those square patch antennas are made of dense dielectric with high relative permittivity. Thus, the antenna prototype in [5] cannot be fabricated by using conventional methods such as etching and engraving. A high gain and low profile antenna structure has been proposed in [6]. Maximum gain and −10 dB impedance bandwidth of the antenna in [6] are 16 dBi and 4.6% of 28 GHz band, respectively. However, the antenna structure in [6] is fabricated from substrate integrated waveguide which cannot be fabricated by using conventional method. Leaf-shaped bowtie antenna is a type of self-complementary printed antenna with low profile and low cost of fabrication. A double sided of leaf-shaped bowtie antenna has been proposed in [7]. Authors in [7] have proposed double sided leaf-shaped bowtie antenna for use in ultra-wideband communication systems in frequency range of 3.0 GHz to 10.5 GHz. Broadside actual gain of the antenna in [7] is from 6.0 dBi to 9.0 dBi. An array of two leaf-shaped bowtie antennas has been proposed in [8]. The antenna structure in [8] has been proposed for use in ultra-wideband communication systems the same as the antenna in [7]. Broadside actual gain of the antenna in [8] is from 5.2 dBi to 8.2 dBi and within frequency range of 4.2 GHz to 10.2 GHz. A linear array of 4 leaf-shaped bowtie slot antennas has been proposed in [9] for use in ultrawide band communication system. Authors in [9] have used two layers of dielectric superstrate to improve actual gain and reflection coefficient of antenna structure. The analysis results showed that −10 dB impedance bandwidth occupies the range of 7.8 GHz to 8.9 GHz and 9.5 GHz to 9.6 GHz. The maximum actual gain in broadside direction is 19.5 dBi at 8.2 GHz and 19.7 dBi at 9.6 GHz. In this paper, a linear array of 4 leaf-shaped bowtie slot antennas is designed and proposed for use in 28 GHz frequency band. Motivation for introducing the slot antennas array are high gain, low profile, and broad impedance bandwidth. In addition, each antenna element can be fed by normal microstrip feedline. Therefore, the antenna structure can be fabricated by using conventional method such as etching and engraving. In previous research [10], planar partially reflecting surface (PRS) has been used to enhance broadside directivity of waveguide aperture an-

Manuscript received April 28, 2021.
Manuscript revised August 19, 2021.
Manuscript publicized September 30, 2021.

[†]The authors are with Graduate School of Information Science and Technology, Hokkaido University, Sapporo-shi, 060-0814 Japan.
a) E-mail: mangseanghor@wtemc.ist.hokudai.ac.jp

DOI: 10.1587/transcom.2021EBP3071

tenna. The concept of multiple reflection between PRS and antenna ground plane has also been introduced in [11]–[13] for gain enhancement. Multiple reflection of electromagnetic wave between PRS and ground plane is in the form of 1-D cavity structure which is also called cavity resonator antenna (CRA). In [14], gain of microstrip antenna has been increased by 2.5 dB after a holey superstrate has been used. In [15], dielectric superstrate has been used to enhance gain and bandwidth of planar antenna instead of PRS. To obtain optimum gain and bandwidth of the planar antenna in [15], distance between dielectric superstrate and the antenna ground plane must be optimized. In this paper, two layers of dielectric superstrate are used to enhance gain and −10 dB impedance bandwidth of linear array of 4 leaf-shaped bowtie slot antennas. In addition to [16] and [9], where leaf-shaped bowtie slot antenna has been proposed for use in ultrawide band communication systems, linear array of 4 leaf-shaped bowtie slot antennas with two layers of dielectric superstrate is introduced for use in quasi-millimeter wave frequency band, in this paper.

The remaining sections of this paper are organized as following. In Sect. 2, structural parameters of the single slot antenna and linear array of slot antennas are presented. In Sect. 3, gain enhancement of the designed slot antennas array is investigated based on the simulated results obtained by FDTD simulation in commercial software (Sim4Life). In Sect. 4, comparison between simulated and measured results is drawn. In Sect. 5, conclusion of this paper is drawn.

2. Design of Leaf-Shaped Bowtie Slot Antennas Array

The principal concept of self-complementary antenna is a natural broad-band antenna with a constant input impedance versus frequency and geometry. From [17], [18], self-complementary antenna has been introduced as an infinite shape, which is difficult to use in real application. Therefore the infinite shape in [17], [18] must be truncated in order to use in real application. Leaf-shaped bowtie antenna, which is proposed by the authors in [7], has been evolved from infinite shape of self-complementary antenna. From [7], Leaf-shaped bowtie slot antenna has been proposed in [16]. In this section, leaf-shaped bowtie slot antenna is employed as radiating element in a linear array for use in 28 GHz frequency band.

2.1 Design of Leaf-Shaped Bowtie Slot Antenna

Figure 1 shows structure of single leaf-shaped bowtie slot antenna in detail. To create a leaf-shaped slot, a square slot is cut on ground plane of a dielectric substrate with the relative permittivity of $\varepsilon_r = 2.17$ and thickness of h. The square slot is rounded by curve line at two corners (90° angle). The side length of square slot is L_e and the radius of the curve line is R_s. The length L_e can be calculated by using the formula from [7] as following:

$$L_e = \frac{\lambda_0}{4\sqrt{\varepsilon_{re}}} \quad ; \quad \varepsilon_{re} = \frac{\varepsilon_r + 1}{2} \tag{1}$$

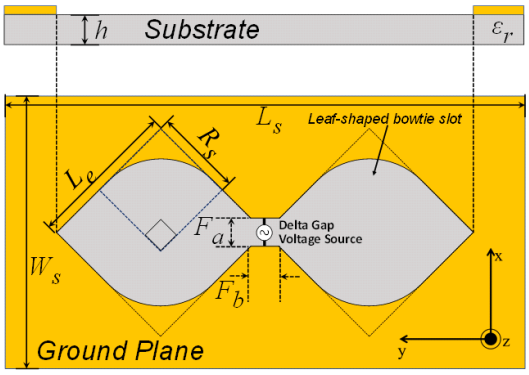

Fig. 1 Structure of leaf-shaped bowtie slot antenna.

Table 1 Structural parameters of leaf-shaped bowtie slot antenna (All dimensions are indicated in mm).

L_e	R_s	L_s	W_s	F_a	F_b	h
2.8	1.7	20	10	0.6	0.6	0.38

In the above formula (1), λ_0 is free-space wavelength at the lower limit frequency of the operating frequency band. Table 1 shows the structural parameters of the single leaf-shaped bowtie slot antenna.

The material, which is used as substrate, has the relative permittivity of $\varepsilon_r = 2.17$, thickness of $h = 0.38$ mm and dissipation factor $\tan\delta = 0.00085$ [19]. The side length L_e is set to 2.8 mm so that the lower limit frequency is about 21 GHz, and the curvature radius R_s is chosen to be $0.6L_e = 1.7$ mm [16].

The impedance of leaf-shaped bowtie slot antenna with the structural parameters listed in the Table 1 are analyzed by Finite-Difference Time-Domain (FDTD) method using commercial simulation software Sim4Life [20]. In the simulation, ideal delta gap voltage source is used as an excitation source as shown in Fig. 1. Gaussian pulse is used to analyze antenna characteristics over broad bandwidth. In the FDTD simulation, grid size of the single slot antenna is set as following, $\Delta x = 0.05$ mm, $\Delta y = 0.05$ mm and $\Delta z = 0.02$ mm. 10 layers of UPML (Uniaxial Perfectly Matched Layer) is employed as boundary condition. Characteristics of the single antenna element are analyzed over frequency range of 27 GHz to 29 GHz.

Figure 2 shows the frequency characteristics of reflection coefficient magnitude $|S_{11}|$ and actual gain of single slot antenna. In the figure, $|S_{11}|$ is calculated with the reference impedance of 110 Ω. From the figure, it can be seen that −10 dB impedance bandwidth occupies the range of 27 GHz to 29 GHz. Actual gain of single slot antenna in the broadside radiation is 7 dBi within 27 GHz and 29 GHz. Fig. 3 and Fig. 4 show the analysis radiation pattern along E-plane and H-plane of single slot antenna which are evaluated at frequencies of 27 GHz, 28 GHz, and 29 GHz. The maximum gain and value of Half-power beamwidth (HPBW) are shown in the caption of Fig. 3 and Fig. 4.

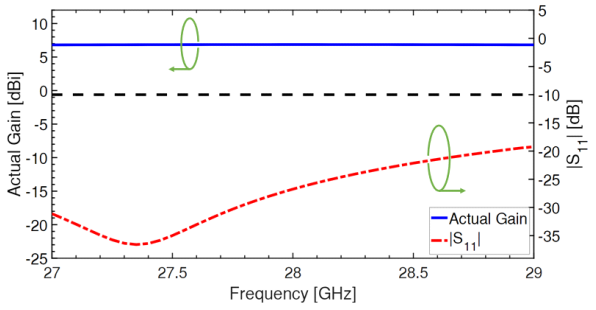

Fig. 2 Characteristics of single leaf-shaped bowtie slot antenna.

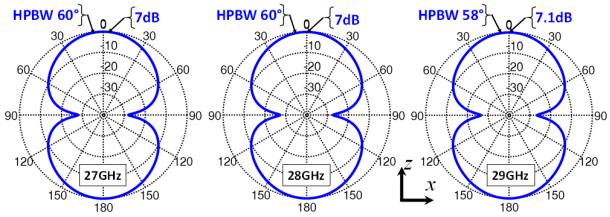

Fig. 3 E-plane pattern of single leaf-shaped bowtie slot antenna.

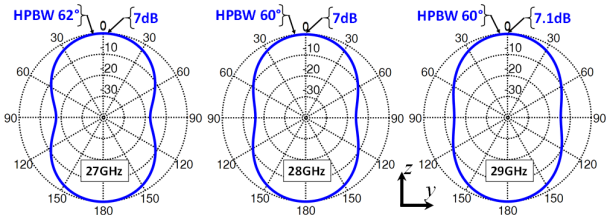

Fig. 4 H-plane pattern of single leaf-shaped bowtie slot antenna.

2.2 Design of Slot Antennas Array with Feedline

By using the leaf-shaped bowtie slot antenna described in Sect. 2.1 as radiating elements of the slot antennas array, a linear array of 4 leaf-shaped bowtie slot antennas is designed for the investigation of gain enhancement with the use of high-permittivity superstrates which will be discussed in Sect. 3. Figure 5 shows the completed structure of the slot antennas array with microstrip feedline. Structural parameters of the designed slot antennas array are shown in Table 2. Conventional microstrip feedline has been used to connect each antenna element to input port with the characteristic impedance of 50 Ω [21]. As shown in Fig. 5, Each end of the microstrip line is connected by conducting probe to the ground plane vicinity of each slot [16]. Each conducting probe has radius R_{probe}. Figure 6 shows structure of conducting probe in detail. Each microstrip line are jointed in pairs by using T-junction. From the T-junction, microstrip tapered line are used for impedance matching and impedance transforming. Finally, each end of the tapered line is connected to 50 Ω input port through T-junction.

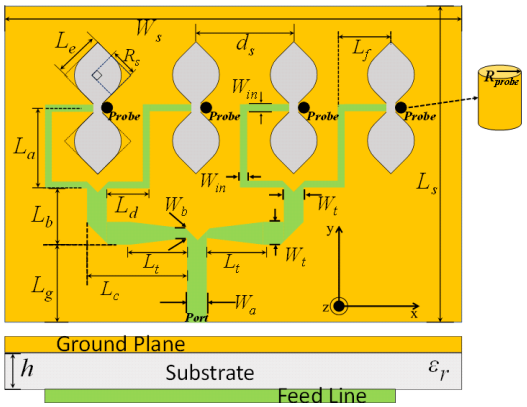

Fig. 5 An array of 4 leaf-shaped bowtie slot antennas.

Table 2 Structural parameters of 4 leaf-shaped bowtie slot antennas array (All dimensions are indicated in mm).

W_s	L_s	L_a	L_b	L_g	L_d	L_t	d_s
58	34	6.6	2.8	7.5	3.9	5.5	8.4
L_f	W_a	W_b	W_t	W_{in}	R_{probe}	L_c	h
3.6	1	0.3	0.8	0.2	0.5	8.3	0.38

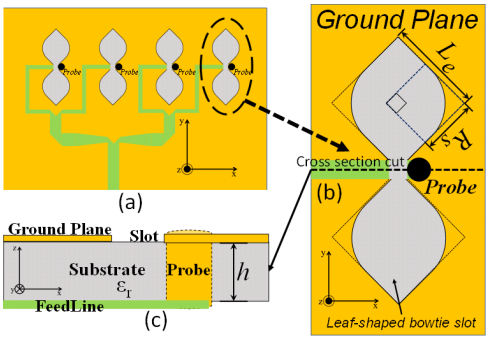

Fig. 6 Structure of conducting probe in connection between feedline and ground plane vicinity of each slot.

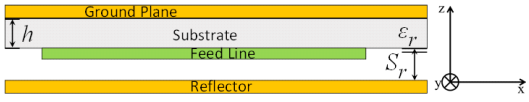

Fig. 7 Side view of an array of 4 leaf-shaped bowtie slot antennas.

2.3 Characteristics of Leaf-Shaped Bowtie Slot Antennas Array without and with Reflector

Leaf-shaped bowtie slot antenna has bidirectional radiation pattern. Thus, a flat reflector is placed under the antenna substrate as shown in Fig. 7 to make the radiation pattern unidirectional. In the following consideration, the distance between the antenna substrate and the reflector is set to $S_r = 2.5$ mm which is about a quarter of free space wavelength at 28 GHz band. In the FDTD simulation, grid size of slot antennas array structure is set as following, $\Delta x = 0.05$ mm, $\Delta y = 0.05$ mm and $\Delta z = 0.02$ mm. 10 layers of UPML (Uniaxial Perfectly Matched Layer) is employed

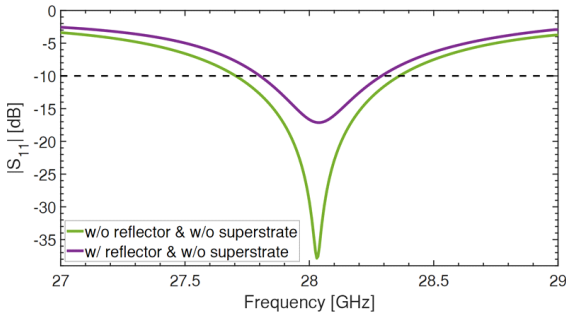

Fig. 8 $|S_{11}|$ comparison between slot antennas array with reflector and without reflector.

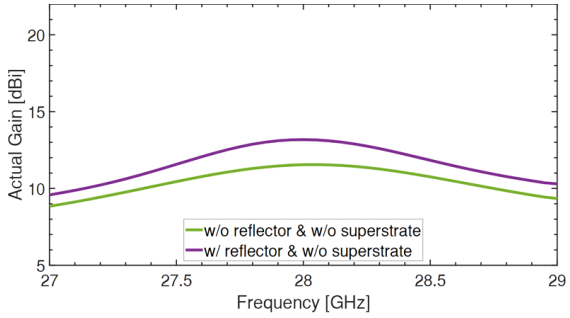

Fig. 9 Actual gain comparison between slot antennas array with reflector and without reflector.

as boundary condition. The antenna characteristics are analyzed in the frequency range of 27 GHz to 29 GHz with sampling frequency of 0.05 GHz. From Fig. 5 leaf-shaped bowtie slot antennas are connected to microstrip feedline to form up an array configuration. Therefore, impedance bandwidth is not as broad as those in Fig. 2 because microstrip feedline is frequency dependence. In addition, as element spacing is changed, feedline is also changed. Thus, antenna element spacing ds is chosen to have an optimum −10 dB impedance bandwidth and actual gain. The analysis results in Fig. 8 show that −10 dB impedance bandwidth of the slot antennas array in Fig. 5 occupies frequency range of 27.7 GHz to 28.36 GHz which is about 660 MHz. However, the −10 dB impedance bandwidth is decreasing after a flat reflector is employed. The −10 dB impedance bandwidth of the slot antennas array with reflector occupies the frequency range of 27.8 GHz to 28.29 GHz which is about 490 MHz. Therefore, −10 dB impedance bandwidth decreases around 170 MHz.

From analysis results in Fig. 9, the slot antennas array without reflector has maximum actual gain of 11.55 dBi and −3 dB gain bandwidth occupies the range of 27 GHz to 29 GHz. In addition, the slot antennas array with reflector has maximum actual gain of 13.17 dBi and −3 dB gain bandwidth occupies the range of 27.17 GHz to 29 GHz. Therefore, maximum actual gain of the slot antennas array increases around 1.62 dBi after the reflector is used. However, −3 dB gain bandwidth decreases around 170 MHz. Figure 10 and Fig. 11 show numerical results of radiation pattern along

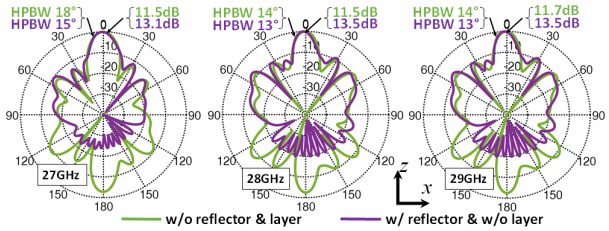

Fig. 10 E-plane pattern comparison between antenna array with reflector and without reflector.

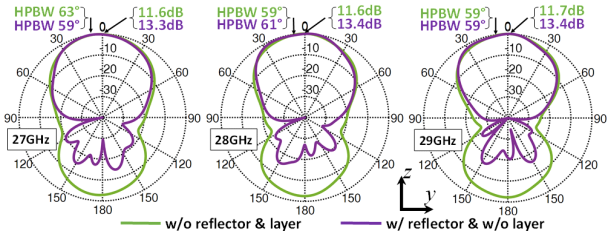

Fig. 11 H-plane pattern comparison between antenna array with reflector and without reflector.

E-plane and H-plane. The numerical results of radiation pattern are evaluated at frequencies of 27 GHz, 28 GHz and 29 GHz. Without reflector, the slot antennas array has bidirectional radiation pattern. Half-power beamwidth (HPBW) along E-plane is 18° at 27 GHz and 14° at 28 GHz and 29 GHz. HPBW along H-plane is 63° at 27 GHz and 59° at 28 GHz and 29 GHz. Sidelobe level is −10 dB at 27 GHz and −8 dB at 28 GHz and 29 GHz along E-plane. From Fig. 10 and Fig. 11, unidirectional radiation pattern is obtained, after a reflector is used. HPBW of the slot antennas array with reflector is 15° at 27 GHz, 13° at 28 GHz and 13° at 29 GHz along E-plane. HPBW of the slot antennas array with reflector is 59° at 27 GHz, 61° at 28 GHz, and 59° at 29 GHz along H-plane. Sidelobe level is −10 dB at 27 GHz, −8 dB at 28 GHz and −7 dB at 29 GHz along E-plane.

3. Gain Enhancement of Leaf-Shaped Bowtie Slot Antennas Array Using High Permittivity Superstrates

3.1 Antennas Array with one Layer of Dielectric Superstrate

From Fig. 8, −10 dB impedance bandwidth is degraded after the flat reflector is placed under the slot antennas array substrate to make radiation pattern unidirectional. From [15], dielectric superstrate with high permittivity can be used to enhance gain and bandwidth of planar antenna.

In this paper, dielectric superstrate is introduced to enhance gain and bandwidth of linear array of 4 leaf-shaped bowtie slot antennas. In the following simulation, the material, which is assumed to be employed as dielectric superstrates, is ROGERS RT/duroidTM 6010LM microwave laminate with a relative permittivity of $\varepsilon_{rs} = 10.2$ and a dissipation factor of $\tan\delta = 0.0023$ [22]. The effectiveness of using dielectric superstrate layer is significantly depend-

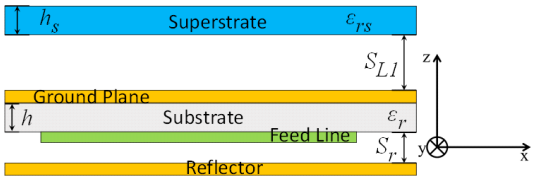

Fig. 12 Side view of antenna structure with one layer of superstrate.

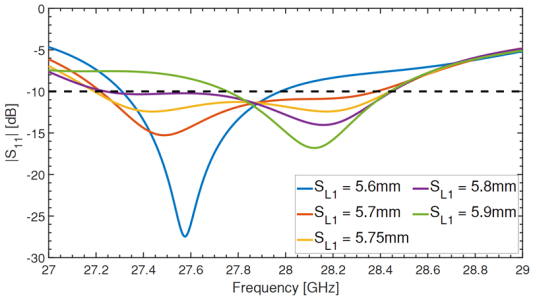

Fig. 13 $|S_{11}|$ comparison by changing distance S_{L1}.

Table 3 Effect of distance S_{L1} on −10 dB bandwidth and maximum actual gain.

S_{L1} (mm)	−10 dB bandwidth	Maximum gain
S_{L1} = 5.6	0.66 GHz (27.31–27.97 GHz)	18.94 dBi
S_{L1} = 5.7	1.16 GHz (27.22–28.38 GHz)	19.2 dBi
S_{L1} = 5.75	1.25 GHz (28.44–27.19 GHz)	19.14 dBi
S_{L1} = 5.8	1.2 GHz (28.44–27.24 GHz)	18.96 dBi
S_{L1} = 5.9	0.68 GHz (28.44–27.76 GHz)	18.39 dBi

ing on distance (S_{L1}) between ground plane and dielectric superstrate layer itself [13]–[15].

Therefore, distance S_{L1} is precisely studied to obtain maximum performance of −10 dB impedance bandwidth and gain of the slot antennas array. Figure 12 shows side view of the antenna structure with one layer of dielectric superstrate on top of the leaf-shaped bowtie slot antennas array designed in the Sect. 2.2. In the following FDTD simulation, setting of grid size of slot antennas array structure is the same as in previous case. However, grid size of dielectric superstrate layer is set as following, Δx = 0.05 mm, Δy = 0.05 mm and Δz = 0.05 mm. Characteristics of the slot antennas array with reflector and one layer of dielectric superstrate are analyzed within the same frequency range and frequency sampling as in Sect. 2.3.

Figure 13 shows the comparison of the frequency response of $|S_{11}|$ by changing distance S_{L1}. From the comparison, the maximum −10 dB impedance bandwidth, which is about 1.25 GHz, is obtained when distance S_{L1} is equal to 5.75 mm. Fig. 14 shows variation of actual gain by changing the distance S_{L1}. The maximum actual gain is obtained at two values of distance S_{L1} (S_{L1} = 5.7 mm, and S_{L1} = 5.75 mm). From both results of −10 dB impedance bandwidth and actual gain, the optimum location of superstrate layer is at S_{L1} = 5.75 mm. Effect of the distance S_{L1} on −10 dB bandwidth and maximum actual gain is summarized in Table 3.

Figure 15 and Fig. 16 show $|S_{11}|$ and actual gain com-

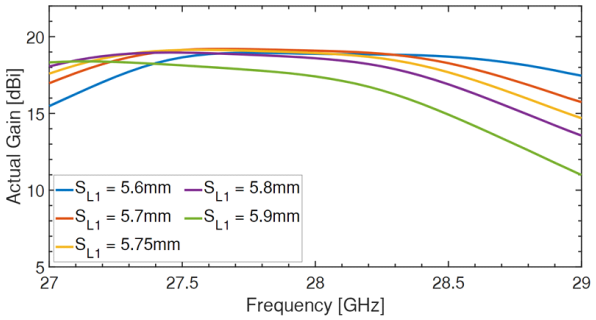

Fig. 14 Actual gains comparison by changing distance S_{L1}.

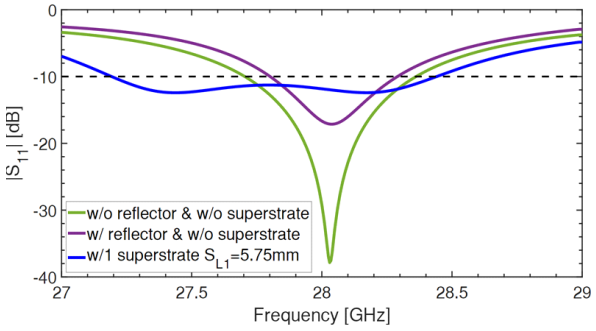

Fig. 15 $|S_{11}|$ comparison after one layer of superstrate is used.

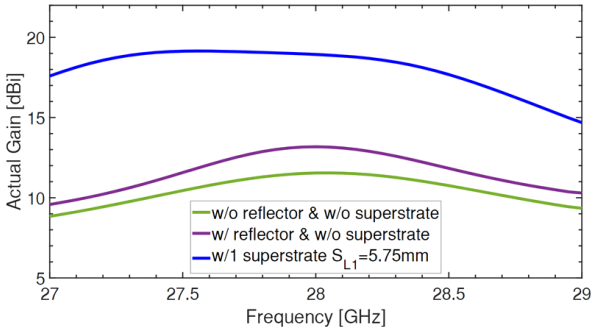

Fig. 16 Actual gain comparison after one layer of superstrate is used.

parison after one layer of dielectric superstrate is placed above the designed slot antennas array which is illustrated in Fig. 12. From Fig. 15, it can be seen that −10 dB impedance bandwidth of the slot antennas array with one layer of dielectric superstrate occupies the frequency range of 27.19 GHz to 28.44 GHz, which is about 1.25 GHz bandwidth. Comparing to the slot antennas array without dielectric superstrate, −10 dB impedance bandwidth increases around 780 MHz after one layer of dielectric superstrate is used.

From Fig. 16, it can be observed that maximum actual gain in broadside is about 19.14 dBi and −3 dB gain bandwidth occupies the frequency range of 27 GHz to 28.77 GHz which is about 1.77 GHz gain bandwidth. Comparing to the case without dielectric superstrate, maximum actual gain has been enhanced around 6 dBi after one layer of dielectric superstrate is used.

Figure 17 and Fig. 18 show the radiation pattern com-

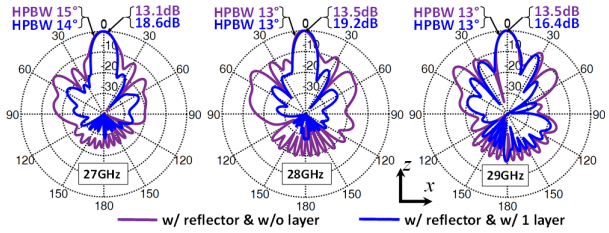

Fig. 17 E-plane pattern comparison after one layer of superstrate is used.

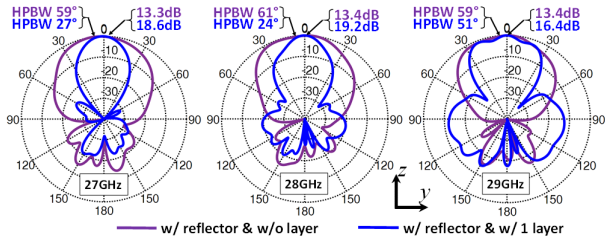

Fig. 18 H-plane pattern comparison after one layer of superstrate is used.

parison of the slot antennas array with one dielectric superstrate layer above the designed slot antennas array as illustrated in Fig. 12. These results are evaluated at frequencies of 27 GHz, 28 GHz and 29 GHz. E-plane and H-plane patterns are shown in Fig. 17 and Fig. 18, respectively. From the figures, it can be confirmed that radiation pattern has been improved after one layer of dielectric superstrate is used. Along E-Plane, sidelobe level is around −20 dB at 27 GHz and 28 GHz and around −10 dB at 29 GHz below the main lobe. HPBW along E-plane is 14° at 27 GHz, 13° at 28 GHz and 13° at 29 GHz. HPBW along H-Plane decreases to 27° at 27 GHz, 24° at 28 GHz and to 51° at 29 GHz.

After one layer of dielectric superstrate is used, sidelobe level and HPBW are getting smaller, and gain tends to be higher at lower frequency. At higher frequency, sidelobe level and HPBW are getting higher, and gain tends to be lower. From [5], maximum gain of the proposed antenna is 16 dBi and impedance bandwidth is from 26.5 GHz to 30.8 GHz which is about 4.3 GHz bandwidth. However, the proposed 4 leaf-shaped bowtie slot antennas array has maximum gain of 19.14 dBi which is 3.14 dBi higher. −10 dB impedance bandwidth of the 4 leaf-shaped bowtie slot antennas array is 1.25 GHz bandwidth which is 3.05 GHz smaller than that of antenna structure in [5]. On the other hand, the process to fabricate antenna prototype in [5] is more complex and higher cost than the process to fabricate 4 leaf-shaped bowtie slot antennas array.

3.2 Antennas Array with 2 Layers of Dielectric Superstrate

To further study the effect of resonant cavity structure, which is created by dielectric superstrate, another dielectric superstrate layer is added on top of the first layer to form up the second resonant cavity structure. Figure 19 shows the side view of antenna structure with 2 resonant cavities. The thickness and material of the second dielectric superstrate

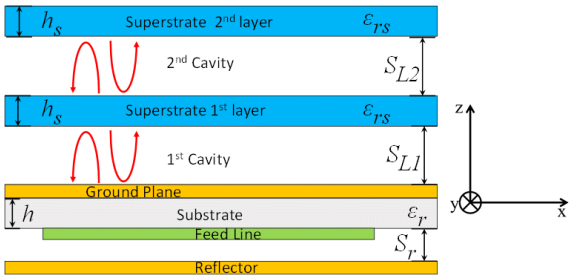

Fig. 19 Side view of antenna structure with two dielectric superstrate layers.

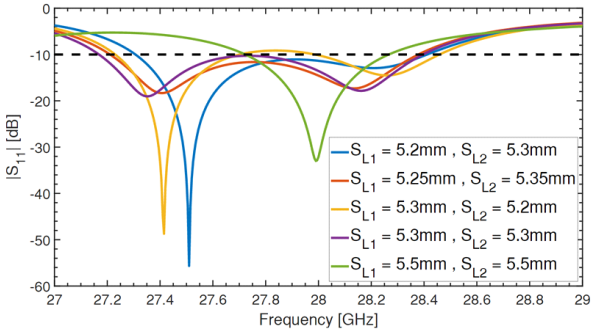

Fig. 20 $|S_{11}|$ comparison by changing distances S_{L1} and S_{L2}.

Table 4 Effect of distances S_{L1} and S_{L2} on −10 dB bandwidth and maximum actual gain.

S_{L1}, S_{L2} (mm)	−10 dB bandwidth	Maximum gain
S_{L1} = 5.2, S_{L2} = 5.3	1.1 GHz (27.31–28.41 GHz)	20.3 dBi
S_{L1} = 5.25, S_{L2} = 5.35	1.16 GHz (27.21–28.37 GHz)	20.44 dBi
S_{L1} = 5.3, S_{L2} = 5.2	0.47 GHz (27.23–27.7 Hz) 0.46 GHz (28.45–27.99 GHz)	20.37 dBi
S_{L1} = 5.3, S_{L2} = 5.3	1.22 GHz (28.39–27.17 GHz)	20.49 dBi
S_{L1} = 5.5, S_{L2} = 5.5	0.54 GHz (27.72–28.26 GHz)	19.29 dBi

layer are identical to those of the first layer; however, in [15], thickness of second superstrate layer is about twice of thickness of first superstrate layer. In addition, the distance between ground plane to the first layer is changed after the second layer is added. To get maximum performance of gain and reflection coefficient, distance S_{L1} and S_{L2} needs to be precisely optimized.

Figure 20 shows the comparison of $|S_{11}|$ by changing distance S_{L1} and S_{L2}. From the analysis results, maximum −10 dB impedance bandwidth is obtained at S_{L1} = 5.3 mm and S_{L2} = 5.3 mm. The maximum −10 dB impedance bandwidth is about 1.22 GHz bandwidth. Figure 21 shows actual gain comparison by changing distance S_{L1} and S_{L2}. Maximum actual gain is obtained at S_{L1} = 5.3 mm and S_{L2} = 5.3 mm. The maximum actual gain is around 20.49 dBi. Effect of the distances S_{L1} and S_{L2} on −10 dB bandwidth and maximum actual gain is summarized in Table 4.

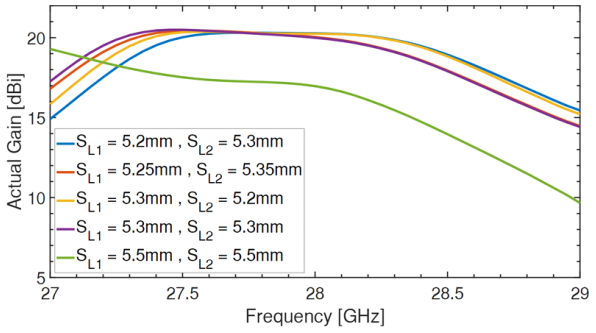

Fig. 21 Actual gains comparison by changing distances S_{L1} and S_{L2}.

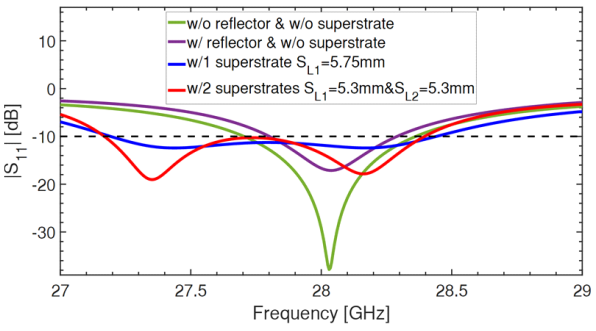

Fig. 22 $|S_{11}|$ comparison with two dielectric superstrate layers.

Figure 22 shows the $|S_{11}|$ comparison, after two layers of dielectric superstrate are arranged on the top of slot antennas array as illustrated in Fig. 19. From the Fig. 22, it can be seen that -10 dB impedance bandwidth of the slot antennas array with two dielectric superstrate layers occupies the frequency range of 27.17 GHz to 28.39 GHz which is about 1.22 GHz. Therefore, after two layers of dielectric superstrate are used, -10 dB impedance bandwidth of the antenna structure is decreased around 30 MHz.

From [23], each mobile operator in Japan has been allocated for a total of 400 MHz bandwidth in 28 GHz frequency band. Therefore, the proposed antenna structure can offer 1.22 GHz of -10 dB impedance bandwidth, which is sufficient for practicality. From Fig. 23, maximum actual gain in the broadside direction is about 20.49 dBi and -3 dB gain bandwidth occupies the frequency range of 27.02 GHz to 28.57 GHz which is about 1.55 GHz. Comparing to the case with one layer of dielectric superstrate, maximum actual gain has been enhanced around 1.35 dBi after two layers of dielectric superstrate are used.

Figure 24 and Fig. 25 show comparison of radiation pattern along E-plane and H-plane, which are evaluated at frequencies of 27 GHz, 28 GHz and 29 GHz after two dielectric superstrate layers are arranged on top of the slot antennas array ground plane with optimized spacings of $S_{L1} = 5.3$ mm and $S_{L2} = 5.3$ mm. After the second dielectric superstrate layer is added, sidelobe level is slightly increasing at 27 GHz and is slightly decreasing at 28 GHz and 29 GHz. On the other hand, maximum gain in the broadside radiation is slightly increasing and HPBW is also slightly decreasing

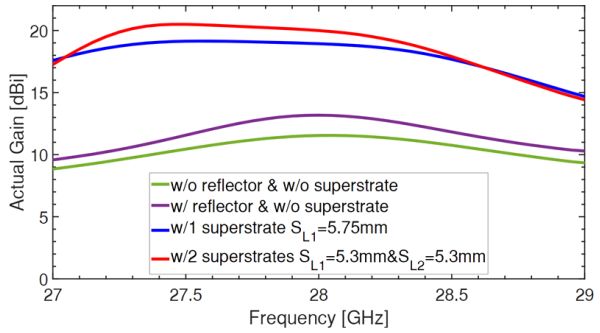

Fig. 23 Actual gain comparison with two dielectric superstrate layers.

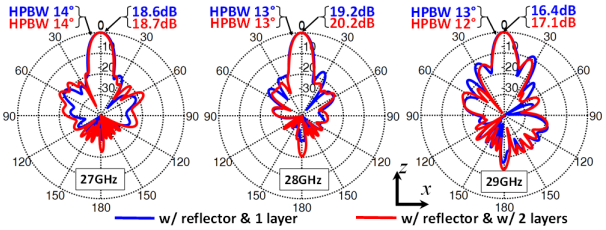

Fig. 24 E-plane pattern comparison with two dielectric superstrate layers.

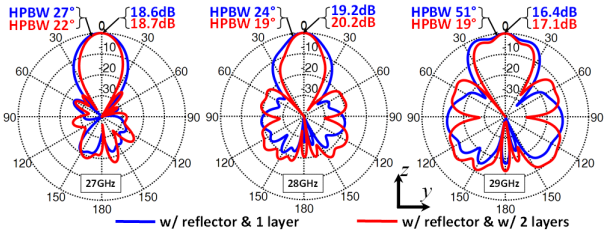

Fig. 25 H-plane pattern comparison with two dielectric superstrate layers.

Table 5 Effect of element spacing d_s on -10 dB bandwidth and maximum actual gain.

d_s	-10 dB bandwidth	Maximum gain
d_s = 8.2 mm	0.34 GHz (27.3–27.64 GHz) 0.6 GHz (28.04–28.64 GHz)	20.4 dBi
d_s = 8.3 mm	0.45 GHz (27.23–27.68 GHz) 0.63 GHz (27.88–28.51 GHz)	20.47 dBi
d_s = 8.4 mm	1.22 GHz (27.17–28.39 GHz)	20.49 dBi
d_s = 8.5 mm	1.18 GHz (27.1–28.28 GHz)	20.49 dBi
d_s = 8.6 mm	1.12 GHz (27.04–28.16 GHz)	20.49 dBi

along H-plane.

Figure 26 and Fig. 27 show comparison of $|S_{11}|$ and actual gain of the slot antennas array with two dielectric superstrate layers by changing element spacing ds. From Fig. 27, analysis results show that actual gain has maximum value at $d_s = 8.4$ mm, $d_s = 8.5$ mm, and $d_s = 8.6$ mm. From Fig. 26, -10 dB impedance bandwidth is maximum at $d_s = 8.4$ mm. Therefore, the optimum element spacing for both -10 dB impedance bandwidth and actual gain is $d_s = 8.4$ mm. Effect of the element spacing d_s on -10 dB bandwidth and maximum actual gain is summarized in Table 5.

Finally, comparison of radiation efficiency is performed

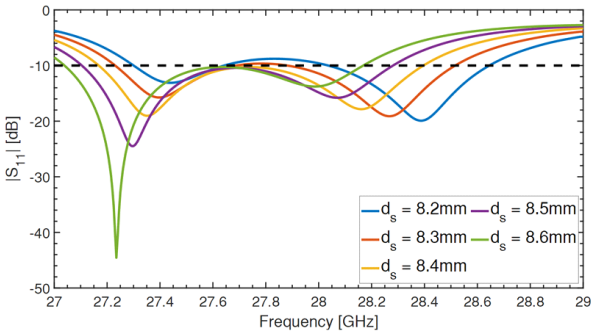

Fig. 26 $|S_{11}|$ comparison by changing element spacing d_s.

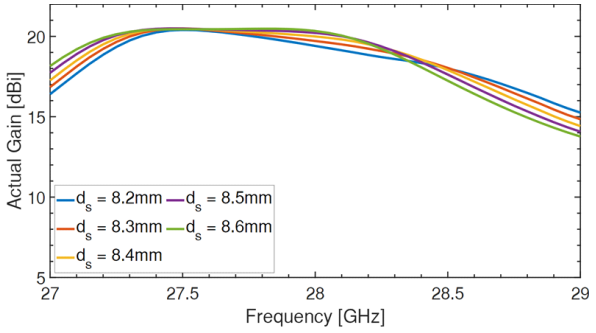

Fig. 27 Actual gains comparison by changing element spacing d_s.

as following. Total radiation, which will be evaluated, are calculated as in following equations from FDTD simulator sim4Life [20]:

$$\eta_{total} = \eta_{rad} \times \eta_{mis} \tag{2}$$

$$\eta_{mis} = \frac{P_{in}}{P_{av}} \tag{3}$$

$$\eta_{rad} = \frac{G_{max}}{D_{max}} \tag{4}$$

In these equations, η_{total} is total radiation efficiency, η_{mis} is mismatch efficiency, η_{rad} is radiation efficiency, P_{in} is total input power, P_{av} is total available power, G_{max} and D_{max} are maximum gain and maximum directivity. Figure 28 shows comparison of total radiation efficiency which is analyzed by FDTD in commercial software Sim4Life. Without using reflector, the array antenna has high total efficiency at 28 GHz and low total efficiency when frequency is getting higher and lower. After a reflector is used, the trend of efficiency is not changed. However, performance of total efficiency is degraded. After one layer of dielectric superstrate is used, total efficiency is enhanced at lower frequency. Total efficiency is within 77% to 91% over 27 GHz to 28.7 GHz. After two layers of dielectric superstrate are used, total efficiency is within 86% to 95% over 27.17 GHz to 28.4 GHz.

4. Simulation and Measurement Comparison

To validate the analysis results in Sect. 3, the prototype of linear array of 4 leaf-shaped bowtie slot antennas is fabricated by using etching and engraving technique for the case

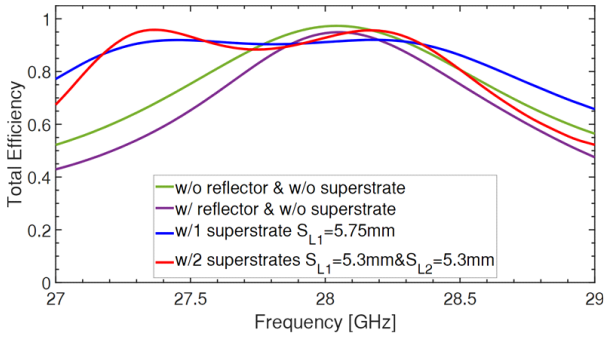

Fig. 28 Total radiation efficiency comparison.

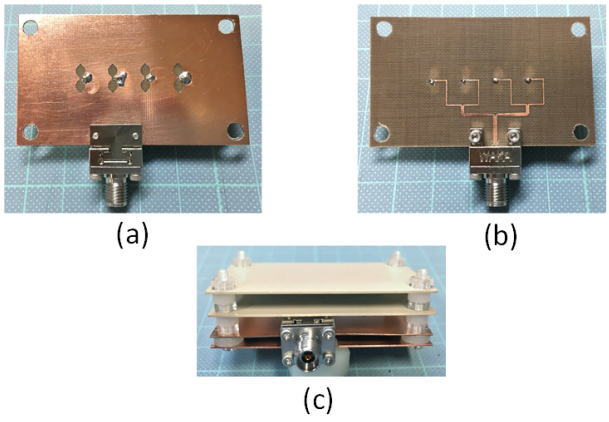

Fig. 29 Prototype of linear array of 4 leaf-shaped bowtie slot antenna. (a) antenna ground plane, (b) antenna feedline, (c) antenna side view with two dielectric superstrate layers.

of $S_{L1} = S_{L2} = 5.3$ mm.

Figure 29 shows prototype of the proposed antenna structure. Figure 30 shows comparison between measured and simulated results. From Fig. 30, the measured −10 dB impedance bandwidth occupies the range of 27.22 GHz to 28.55 GHz, and the simulated −10 dB impedance bandwidth occupies the range of 27.17 GHz to 28.39 GHz. Therefore, the measured −10 dB impedance bandwidth is slightly shifting to higher frequency band. However, the discrepancies between the measured and simulated −10 dB impedance bandwidth are small. In addition, −10 dB impedance bandwidth is still in the same 28 GHz band. From Fig. 30, the measured actual gain is around 1.5 dBi smaller than simulated actual gain at 28 GHz. The discrepancies could be due to the conductor loss, fabrication error of the prototype antenna, and the disturbance of radiation characteristics which is caused by screws or connectors.

Figure 31 and Fig. 32 show comparison between measured and simulated radiation pattern at frequencies of 27.2 GHz, 27.5 GHz, 28 GHz, and 28.5 GHz, which are within −10 dB impedance bandwidth (27.2 GHz–28.5 GHz). In broadside direction, there are small discrepancies between measured and simulated results at 28.5 GHz along both E-plane and H-plane. However, sidelobe level of measured radiation pattern along E-plane is slightly increasing at

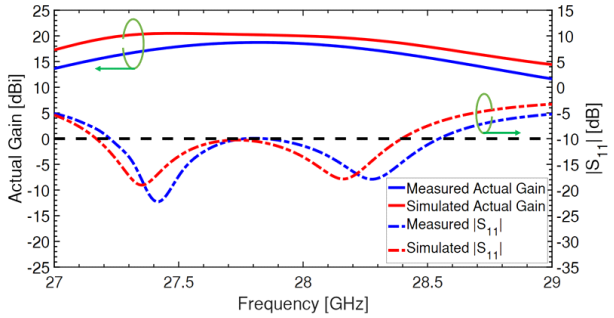

Fig. 30 Comparison between measured and simulated results for reflection coefficient $|S_{11}|$ and actual gain.

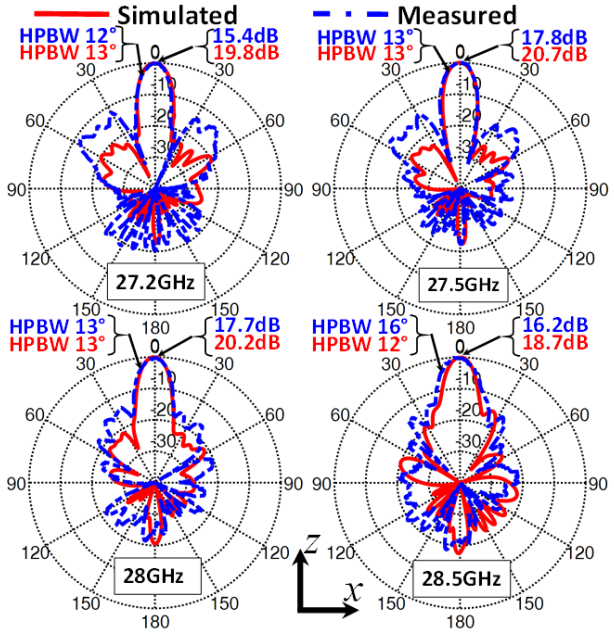

Fig. 31 Comparison between measured and simulated E-plane pattern.

27.2 GHz, 27.5 GHz and 28 GHz. From Fig. 31 and Fig. 32 maximum gain of measured radiation pattern at 28 GHz is around 2 dB smaller than the maximum gain of simulated radiation pattern. The discrepancies could be due to the fabrication error of the prototype antenna, and the disturbance of radiation characteristics which is caused by screws or connectors. In terms of HPBW, Fig. 31 and Fig. 32 show a good agreement between simulated and measured radiation patterns along both E-plane and H-plane. Therefore, both simulated and measured results confirm that the proposed antenna structure has good radiation pattern within 27.2 GHz to 28.5 GHz.

5. Conclusion

In this paper, a linear array of 4 leaf-shaped bowtie slot antennas with two layers of dielectric superstrate is proposed for use in quasi-millimeter wave frequency. The antenna characteristics are investigated by FDTD analysis in commercial simulation software (Sim4Life). Actual gain and −10 dB

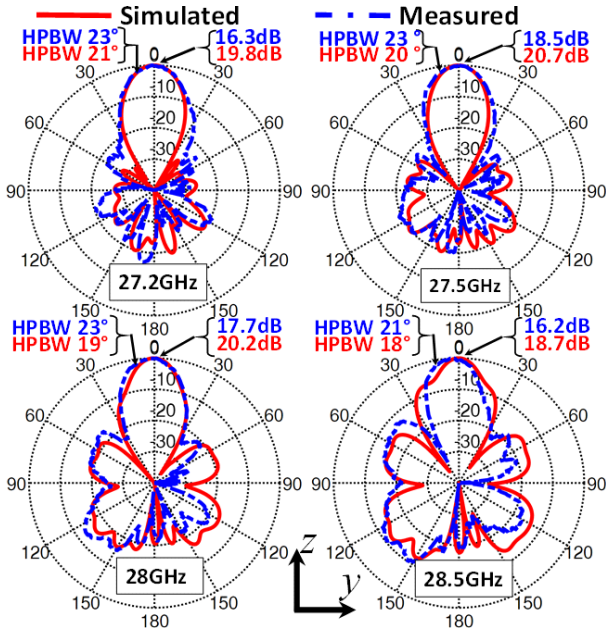

Fig. 32 Comparison between measured and simulated H-plane pattern.

impedance bandwidth of the slot antennas array are improved by using two layers of dielectric superstrate. However, performance of impedance bandwidth is highly associated with location of dielectric superstrate layer. From analysis results, maximum performance of antenna characteristics is obtained when distance S_{L1} is equal to 5.3 mm and S_{L2} is equal to 5.3 mm. The maximum −10 dB impedance bandwidth is 1.22 GHz, which occupies frequency range of 27.17 GHz to 28.39 GHz. Maximum actual gain in broadside direction is 20.49 dBi and −3 dB gain bandwidth is 1.55 GHz, which occupies frequency range of 27.02 GHz to 28.57 GHz. Total efficiency of proposed antenna structure is between 86% to 95% over operational impedance bandwidth. The proposed antenna structure has high efficiency and high actual gain. The −10 dB impedance bandwidth of proposed antenna structure is sufficient for future 5G application [23]. In addition, the antenna structure is low cost and easy to fabricate. To validate the analysis results, prototype of the proposed antenna has been fabricated and characteristics of the antenna prototype are measured and compared with simulated results.

Acknowledgments

This study was supported in part by Ministry of Education, Science, Sports and Culture, Fund for the Promotion of Joint International Research, Fostering Joint International Research (B) (18KK0277).

References

[1] B. Raaf, W. Zirwas, K. Friederichs, E. Tiirola, M. Laitila, P. Marsch, and R. Wichman, "Vision for beyond 4G broadband radio systems," 2011 IEEE 22nd International Symposium on Personal, Indoor and Mobile Radio Communications, Sept. 2011. DOI: 10.1109/

PIMRC.2011.6139944
[2] H. Zhao, R. Mayzus, S. Sun, M. Samimi, J.K. Schulz, Y. Azar, K. Wang, G.N. Wong, F. Gutierrez, and T.S. Rappaport, "28 GHz millimeter wave cellular communication measurements for reflection and penetration loss in and around buildings in New York City," Proc. 2013 IEEE International Conference on Communications (ICC), pp.5163–5167, Nov. 2013. DOI: 10.1109/ICC.2013.6655403
[3] A. Ghosh, T.A. Thomas, M.C. Cudak, R. Ratasuk, P. Moorut, F.W. Vook, T.S. Rappaport, G.R. MacCartney, S. Sun, and S. Nie, "Millimeter-wave enhanced local area systems: A high-data-rate approach for future wireless networks," IEEE J. Sel. Areas Commun., vol.32, no.6, pp.1152–1163, June 2014. DOI: 10.1109/JSAC.2014.2328111
[4] T.S. Rappaport, S. Sun, R. Mayzus, H. Zhao, Y. Azar, K. Wang, G.N. Wong, J.K. Schulz, M. Samimi, and F. Gutierrez, "Millimeter wave mobile communications for 5G cellular: It will work!," IEEE Access, vol.1, pp.335–349, May 2013. DOI: 10.1109/ACCESS.2013.2260813
[5] M. Asaadi and A. Sebak, "Gain and bandwidth enhancement of 2×2 square dense dielectric patch antenna array using a holey superstrate," IEEE Antennas Wireless. Propag. Lett., vol.16, pp.1808–1811, March 2017. DOI: 10.1109/LAWP.2017.2679698
[6] M. Asaadi and A. Sebak, "High-gain low-profile circularly polarized slotted SIW cavity antenna for MMW applications," IEEE Antennas Wireless Propag. Lett., vol.16, pp.752–755, Aug. 2016. DOI: 10.1109/LAWP.2016.2601900
[7] M. Ameya, M. Yamamoto, T. Nojima, and K. Itoh, "Leaf-shaped element bowtie antenna with flat reflector for UWB applications," IEICE Trans. Commun., vol.E90-B, no.9, pp.2230–2238, Sept. 2007.
[8] Y. Ito, M. Ameya, M. Yamamoto, and T. Nojima, "Unidirectional UWB array antenna using leaf-shaped bowtie elements and a flat reflector," IET Electorn. Lett., vol.44, no.1, pp.9–11, Jan. 2008. DOI: 10.1049/el:20082741
[9] T. Makanae and M. Yamamoto, "A Study on gain enhancement of a leaf-shaped bowtie slot antenna array employing dielectric superstrates," 2019 International Symposium on Antennas and Propagation, TA1D, Oct. 2019.
[10] G.V. Trentini, "Partially reflecting sheet arrays," IRE Trans. Antennas Propag., vol.4, no.4, pp.666–671, Oct. 1956. DOI: 10.1109/TAP.1956.1144455
[11] A.P. Feresidis, G. Goussetis, S. Wang, and J.C. Vardaxoglou, "Artificial magnetic conductor surfaces and their application to low-profile high-gain planar antennas," IEEE Trans. Antennas Propag., vol.53, no.1, pp.209–215, Jan. 2005. DOI: 10.1109/TAP.2004.840528
[12] A.P. Feresidis and J.C. Vardaxoglou, "High gain planar antenna using optimised partially reflective surfaces," IEE Proc., Microw. Antennas Propag., vol.148, no.6, pp.345–350, Dec. 2001. DOI: 10.1049/ip-map:20010828
[13] A.R. Weily, T.S. Bird, and Y.J. Guo, "A reconfigurable high-gain partially reflecting surface antenna," IEEE Trans. Antennas Propag., vol.56, no.11, pp.3382–3390, Nov. 2008. DOI: 10.1109/TAP.2008.2005538
[14] J.H. Kim, C.H. Ahn, and J.K. Bang, "Antenna gain enhancement using a holey superstrate," IEEE Trans. Antennas Propag., vol.64, no.3, pp.1164–1167, March 2016. DOI: 10.1109/TAP.2016.2518650
[15] M.A. Al-Tarifi, D.E. Anagnostou, A.K. Amert, and K.W. Whites, "Bandwidth enhancement of the resonant cavity antenna by using two dielectric superstrates," IEEE Trans. Antennas Propag., vol.61, no.4, pp.1898–1908, April 2013. DOI: 10.1109/TAP.2012.2231931
[16] S. Fujita, M. Yamamoto, and T. Nojima, "A study of a leaf-shaped bowtie slot antenna for UWB applications," Proc. 2012 International Symposium on Antennas and Propagation, 3B3-1, pp.830–833, Nov. 2012.
[17] Y. Mushiake, "Self-complementary antennas," IEEE Antennas Propag. Mag., vol.34, no.6, pp.23–29, Dec. 1992. DOI: 10.1109/74.180638
[18] Y. Mushiake, "A report on Japanese development of antennas: from the Yagi-Uda antenna to self-complementary antennas," IEEE Antennas Propag. Mag., vol.46, no.4, pp.47–60, Aug. 2004. DOI: 10.1109/MAP.2004.1373999
[19] https://rogerscorp.com/advanced-connectivity-solutions/diclad-series-laminates/diclad-870-880-laminates
[20] https://zmt.swiss/sim4life/
[21] D.M. Pozar, Microwave Engineering, John Wiley & Sons, 2011.
[22] https://rogerscorp.com/advanced-connectivity-solutions/rt-duroid-laminates/rt-duroid-6006-and-6010-2lm-laminates
[23] https://www.ntt-review.jp/archive/ntttechnical.php?contents=ntr202012fa13.html

Mangseang Hor received the B.E. in electrical and electronic engineering from Institute of Technology of Cambodia in 2014. He graduated in M.E. from Electric Department, Chulalongkorn University in 2017. He is currently a Ph.D. student at Graduate School of Information and Science Technology, Hokkaido University. He is a student member of IEICE.

Takashi Hikage received the B.E., M.E., and Ph.D. degree in electronics and information engineering from Hokkaido University, Sapporo, Japan, in 1997, 1999, and 2002. From 1999 to 2003, he was with the Graduate School of Engineering. He is currently an assistant professor at the Graduate School of Information Science and Technology. He is a member of IEICE and IEEE.

Manabu Yamamoto received the B.E., M.E., and Ph.D. degrees in electronics and information engineering from Hokkaido University in 1993, 1995 and 1998. From 1998 to 2003, he was with the Graduate School of Engineering, and is now an associate professor at the Graduate School of Information Science and Technology. His research interests are analysis and design of millimeter-wave antennas and microstrip antenna. He is a member of IEICE and IEEE.